# Integration of Different Permeability Model Parameters for Permeability Prediction from Capillary Pressure Curves in Carbonate Reservoirs

Mustafa Rezaei*[a]

[a] Geoscience Department, Mississippi State University, Starkville, 39759, USA

Mr2509@msstate.edu

*This is a non-peer reviewed preprint submitted to EarthArXiv.*

## Abstract

Permeability prediction is essential for reservoir characterization, commonly derived from core analysis and mercury injection capillary pressure (MICP) data. Many conventional models, often calibrated for sandstones, are based on parameters such as porosity or specific mercury saturation points, which limits their accuracy in carbonate reservoirs due to differing rock properties. This study addresses these limitations by integrating parameters from 12 existing permeability estimation models and selecting three reliable models for carbonates: Swanson's, Winland's, and Pittman's models. These models incorporate Swanson's parameter (maximum Sb/Pc, where $S_b$ is non-wetting phase saturation and Pc is capillary pressure), pore-throat radius at specific saturations (Winland's rx), and porosity (Pittman's model). An integrated framework was developed using data from 50 carbonate samples and validated with 20 additional samples and log data. The permeability values range from 0.01 to 450 millidarcies (mD), with porosity from 1% to 30%. Multiple linear regression established robust relationships between permeability, porosity, and Swanson's parameter, improving prediction accuracy. Validation using MICP and

Stoneley wave data confirmed the model's reliability, demonstrating significant advancements in permeability estimation for heterogeneous carbonate systems. This approach offers a comprehensive and accurate tool for reservoir characterization.

**Keywords**

Permeability Model, Carbonate Reservoir, Permeability Prediction, Mercury Injection, Reservoir Characterization

## 1. Introduction

The extraction of subsurface oil and gas resources depends on several essential factors, such as porosity, permeability, relative permeability (RP), capillary pressure, and wettability, among others (Feng et al., 2021). The permeability of rock is closely associated with the distribution of pore throat sizes, making the mercury injection capillary pressure (MICP) curve a reliable tool for predicting permeability. The RP curve illustrates the relationship between the permeabilities of various fluid phases, including oil and water, within a porous medium. This relationship governs the movement of these phases through the reservoir's porous structure and fracture networks, playing a crucial role in enhancing the precision of reservoir simulation models (Wang et al., 2023). The RP curve plays a vital role in reservoir modeling, as it greatly influences history matching, the development and optimization of production strategies, and enhanced recovery. Therefore, it is essential to develop efficient and precise techniques for obtaining RP curves.

Various techniques have been employed to obtain RP curves, generally classified into direct and indirect methods. The direct approach involves conducting laboratory experiments on rock cores using either steady-state or unsteady-state measurement techniques (Swanson, 1981; Pittman,

1992; Dasidar et al., 2007; Krevor et al., 2012; Chen et al., 2014; Feng et al., 2018). One commonly used technique is mercury injection, where mercury is introduced into the microscopic pores of a porous medium under controlled pressure conditions, establishing a correlation between pressure and the volume of injected mercury. The RP curves derived from these experiments are influenced by the complex micro-pore structure of the medium. Due to the ease of data acquisition and the ability to analyze relatively large sample sizes, numerous researchers have developed RP models based on capillary pressure experiments (Purcell, 1949; Burdine, 1953; Corey, 1954; Brooks and Corey, 1966). Purcell (1949) introduced a permeability model based on the capillary pressure curve, assuming that water flows through smaller capillary tubes while gas moves through larger ones, leading to a straightforward RP model. Expanding on Purcell's foundation, Burdine (1953), Corey (1954), and Brooks and Corey (1966) developed RP models that incorporate pore size distribution and tortuosity; however, these models do not account for the presence of an irreducible water film. The integration of percolation theory into RP calculations, first introduced by Helba et al. (1992), has since been adopted and refined by several researchers, including Salomao (1997), Dixit et al. (1998), Phirani et al. (2009), and Kadet and Galechyan (2014). One of the primary challenges in this approach is accurately determining coordination numbers and pore fractions within network models. Currently, many permeability models rely on the MICP curve, which can be categorized into two main types (Comisky et al., 2007). The first category includes permeability models based on percolation theory, which assumes that flow paths in porous media can be represented by a single-scale aperture. Notable examples within this category are the Kozeny-Carman model (Schwartz et al., 1989; Bernabé and Maineult, 2015), the Katz-Thompson models (Katz and Thompson, 1986), and the Revil-Glover-Pezard-Zamora model (Glover et al., 2006). The second category includes

permeability models based on Poiseuille's equation and Darcy's law, which conceptualize flow paths in porous media as a collection of capillary tubes. Notable models in this category include the Purcell model (Purcell, 1949; Zhang et al., 2017), the Thomeer model (Thomeer, 1960, 1983), the $r_{35}$ model (initially proposed by Winland and later reported by Kolodzie, 1980), the Swanson model (Swanson, 1981; Kamath, 1992), the $r_{25}$ model (Pittman, 1992), the Capillary-Parachor model (Guo et al., 2004; Liu et al., 2016; Xiao et al., 2017), the Huet model (Huet et al., 2005), the r50 model (Rezaee et al., 2006; Gao and Hu, 2013), and the rwgm model (Dastidar et al., 2007), where rwgm represents the weighted geometric mean radius. Zhou et al. (2023) applied the ensemble Kalman method to predict RP curves using saturation data, while Lanetc et al. (2024) developed a novel approach that integrates hybrid pore network and fluid volume methods for RP curve estimation. Additionally, Rezaei et al. (2020) focused on modifying permeability models initially designed for sandstones to enhance their applicability to carbonate reservoirs. While these studies have made notable progress in acquiring RP curves through various methodologies, each approach presents certain limitations. Therefore, the development of a more efficient framework for obtaining RP curves remains a critical objective. Various permeability models, including those developed by Winland (1992), Swanson (1981), and Dastidar (2007), have utilized different parameters to predict permeability, often calibrated using clastic or carbonate rock samples. Carbonate rocks, due to their diverse depositional environments and complex diagenetic processes, pose significant challenges for permeability modeling. Earlier models, such as those by Winland, Pittman, and Swanson, were designed for specific facies and diagenetic conditions, incorporating factors like pore throat size, porosity, and Swanson's parameter—the maximum ratio of Sb/Pcmax.

Although these models have contributed to permeability predictions, they have sometimes exhibited inaccuracies when applied to certain carbonate samples (Nooruddin et al., 2014). To

address these shortcomings, this study introduces a new model that integrates multiple key parameters to improve permeability estimation in carbonate rocks. The proposed model includes porosity, permeability, the pore-throat radius at 35% mercury saturation, and Swanson's parameter, offering a more comprehensive approach. By considering a wider range of influential factors, this model aims to enhance the accuracy and reliability of permeability predictions for complex carbonate reservoirs.

## Materials and Methods

### 2.1 Sample Description and methos

This study utilized 70 core plug samples obtained from three wells within a carbonate reservoir. Each core plug measured one inch in diameter and two inches in length. MICP tests were performed on all samples, where mercury was injected under increasing pressure, and mercury saturation was plotted against pressure. The resulting capillary pressure curves were used to derive key petrophysical properties, including pore-throat sizes and porosity. After a thorough evaluation of various models, three models demonstrating the best integration were selected. Three established permeability prediction models—Winland, Pitman, and Swanson—were evaluated against laboratory-measured permeability values. Permeability was determined using air permeability measurements based on Darcy's law, with values ranging from 0.01 mD to 450 mD, and porosity ranging between 1% and 30%. The MICP test provided porosity calculations by measuring the volume of injected mercury. A multiple linear modeling approach was applied to propose an empirical relationship between permeability and MICP data. Linear regression, combined with laboratory-measured permeability, was used to refine the prediction models, quantifying the relationship between key variables and permeability. This approach ensured the

model's simplicity, interpretability, and improved accuracy through validation against actual permeability data. A permeability log derived from Stoneley waves and 20 Modular Formation Dynamics Tests (MDT) were also incorporated to validate the results. The comparison between predicted and measured permeability values demonstrated the robustness of the proposed model, enhancing its reliability for permeability estimation in carbonate reservoirs.

## 2.2 MICP-based permeability prediction models

Over the years, numerous models for estimating permeability based on MICP curves have been developed. Purcell (1949) introduced a method to calculate permeability by assuming that the porous medium consists of disconnected capillary tubes of uniform length. Thomeer (1983) observed that MICP curves resemble a hyperbolic shape in log-log plots and proposed a permeability estimation model using three parameters derived from the hyperbola. Winland (referenced in Kolodzie, 1980) established an empirical relationship involving $r_{35}$ , permeability, and porosity. Swanson (1981) suggested that the pore space at the hyperbolic curve's inflection point represents the effective pore throat that controls fluid flow. He developed an empirical model linking permeability to the ratio of saturation to capillary pressure ($S_b$ / $P_c$) at this critical point. Pittman (1992) refined this approach by analyzing multiple regression relationships between permeability, porosity, and $r_x$, where x ranged from 10% to 75% of non-wetting phase saturation, with $r_{25}$ providing the strongest correlation. Guo et al. (2004) identified a significant correlation between permeability and the Capillary-Parachor parameters, specifically the maximum value of $S_b/P_c$ . Gao and Hu (2013) demonstrated that permeability could be estimated using $r_{50}$ alone. Liu et al. (2016) enhanced the accuracy of permeability prediction models by incorporating the Capillary-Parachor parameter alongside porosity. Subsequently, Xiao et al.

(2017) suggested dividing samples, such as those from Liu et al.'s (2016) study, into distinct groups based on porosity and developing separate permeability models for each group.

Drawing on the overviews of permeability prediction models provided by Comisky et al. (2007), Nooruddin et al. (2014), and Rashid et al. (2015), we expanded the range of models based on MICP curves by incorporating additional models from more recent studies. The updated summary is presented in Table 1, which includes various parameters derived from MICP curves. These parameters consist of $S_b$, $G$, $P_d$, the Swanson parameter (denoted as s), the Capillary-Parachor parameter (*denoted as cp*), $r_{10}$, $r_{25}$, $r_{35}$, $r_{50}$, $r_{wgm}$, $S_{wirr}$, and λ.

Table 1. Permeability Models Derived from MICP Data.

| Lithology | Model | Equation |
|---|---|---|
| Sandstone | Purcell (1949) | $K = \frac{(\sigma\ Cos\ \theta)^2 F\phi}{2\times 10^4}\int_0^{100}\frac{d\ S_{nw}}{p_c^2}$ |
| Sandstone | Swanson (1981) | $K = 399\ (\frac{S_b}{P_C})_A^{1.691}$ |
| Sandstone | Thomeer (1983) | $K = 3.8068\ G^{-1.3334}(\frac{S_{nw}}{P_d})^2$ |
| Sandston and carbonate | Winland (Kolodzie, 1980) | $K = 49.0316 r_{35}^{1.7007}\phi^{1.4694}$ |
| Sandston | Pittman (1992) | $lgk = -1.221 + 1.415 log\phi + 1.512 lgr_{25}$ |
| Sandston | Capillary-Parachor (Guo et al., 2004) | $k = 0.00007\ (\frac{S_{nw}}{P_c^2})_{cp}^2$ |
| Sandston and Carbonate | Huet et al. (2005) | $k = 1017003(1 - S_{wirr})^{0.5475}\phi^{1.6498}\frac{1}{P_d^{1.7846}}\left[\frac{\lambda}{\lambda+2}\right]^{1.6745}$ |
| Carbonate | Rezaee et al. (2006) | $lgk = -1.16 + 1.78 lg\phi + 0.93 lgr_{50}$ |
| Sandston | Dastidar et al. (2007) | $lgk = -2.51 + 3.06 lg\phi + 1.64 lgr_{wgm}$ |

| | | |
|---|---|---|
| Tight Sandston | Rezaee et al. (2012) | $lgk = -1.92 + 0.949lg\phi + 2.18lgr_{10}$ |
| Sandston and carbonate | Gao and Hu (2013) | $lgk = 0.214 + 2.225lgr_{50}$ |
| Sandston | Liu et al. (2016) | $k = 10^{-5.129}\phi^{3.141}(\frac{S_{nw}}{P_c^2})_{cp}^{0.875}$ |

Where k is permeability, ϕ is porosity, $P_c$ is capillary pressure, $S_b$ is the non-wetting phase saturation, and F is the formation factor. The Swanson parameter represents the maximum value of $S_b/P_c$, and the Capillary-Parachor parameter represents the maximum value of $S_b/P_c^2$. G is the pore geometry factor in the Thomeer model, while $S_b$ is the non-wetting phase saturation when $P_c$ approaches infinity, and $P_d$ is the displacement pressure. G, $S_b$, and $P_d$ can be derived by fitting the MICP curve using the Thomeer model (Thomeer, 1960, 1983). $S_{wirr}$ is the irreducible wetting phase saturation, and λ is the Brooks-Corey index for pore throat size distribution, which can be obtained by fitting the MICP curve using the Brooks-Corey model (Brooks and Corey, 1966). $r_x$ is the pore-throat radius at x% non-wetting saturation, and $r_{wgm}$ is the weighted geometric mean radius, and np is the number of pore throat radii.

The pore throat sizes at the point where the maximum value of $S_b/P_c$ occurs are crucial for effectively connecting the major pore spaces. The $S_b$ at this point reflects the portion of the pore space that predominantly contributes to fluid flow (Swanson, 1981). As a result, the Swanson parameter is expected to have a strong correlation with permeability. The point of maximum $S_b/P_c^2$ provides significant insights into the distribution of effective pore throat sizes. Additionally, the Capillary-Parachor parameter demonstrates a positive correlation with permeability (Guo et al., 2004). $P_d$ represents the minimum capillary pressure required for a non-wetting fluid to penetrate a pore space previously saturated with a wetting fluid. In sandstone reservoirs, lower values of $P_d$ are generally observed in rocks with more uniform particles, fewer cementing materials, and better porosity and permeability (Luo and Wang, 1986). Furthermore, $r_x$ and $r_{wgm}$, which are characteristic parameters of the pore throat size distribution, typically show a positive relationship with permeability (Rezaee et al., 2006, 2012; Dastidar et al., 2007).

## 3. Results and Discussion

After investigating and analyzing various permeability models, we aimed to develop a comprehensive model that incorporates multiple factors, making it more applicable to carbonate reservoirs, which often present challenges due to diagenesis and the complexity of permeability prediction. Following extensive evaluation, we determined that integrating the Winland, Pittman, and Swanson formulas yielded the most accurate and reliable results for carbonate samples. The reason for utilizing these models lies in their well-integrated factors, which complemented each other effectively. As demonstrated in this study, the newly proposed model, developed through the integration of these formulas, has been tested against actual permeability data derived from MICP and log data. The results indicate that the proposed model provides a strong and reliable prediction of permeability.

### 3.1 Winland Permeability Model

Winland (1992) established an empirical relationship between porosity, permeability, and the diameter of pore throats, considering the radius of the pore-throat at 35% mercury saturation (R35). This relationship provides a framework for predicting permeability based on porosity and pore-throat characteristics. The correlation between predicted and measured permeabilities is illustrated in Fig. 2a.

### 3.2 Pittman Permeability Model

Pitman (1992) permeability model was constructed and calibrated using the relationship between porosity, permeability, and the radius of the pore-throat at 25% mercury saturation (R25). The comparison between permeability predictions from the model and actual measured permeability data shows a strong correlation. The results, along with the coefficient of determination ($R^2$), are presented in Fig. 2b.

### 3.3 Swanson Permeability Model

Swanson permeability model incorporates the Swanson's parameter—the maximum ratio of *Sb/Pcmax* to predict permeability. The comparison between predicted and measured permeability values, along with their linear modeling, is illustrated in Fig. 2c, demonstrating the effectiveness of the model.

### 3.3 Model Development and Validation

The development of the new permeability prediction model was guided by a thorough review of existing models, finally after careful consideration we integrated Winland, Swanson and Swanson. Key parameters, characterized by significant coefficients and substantial geological influence on permeability, were prioritized. After integrating these factors, the model underwent rigorous testing to optimize its accuracy.

#### 3.3.1 Proposed Model

Based on samples from carbonate formations and using multiple linear modeling analysis, a new model is introduced here. This model incorporates a comprehensive set of influential factors for permeability estimation in carbonate reservoirs. The model is calibrated for a permeability range up to 90 mD. The advantage of this model lies in its integration of various criteria and factors, offering improvements over previously proposed models. The model was developed using multiple linear modeling analysis and is presented as follows:

$$K = 0.242 - 19.552\,(\log \varphi) - 17.432\,(\log R35) + 3.123\,(\frac{Sb}{Pc}\max)$$

where $R_{35}$ is the radius of the pore-throat related to the 35 % of mercury saturation, K is permeability (mD), $\boldsymbol{\varphi}$ is porosity (%), and Sb/Pcmax is the maximum value of Sb/Pc (Swanson's parameter).

The predicted permeability values versus the actual permeabilities, along with their linear regression model, are presented in Fig. 2d. The linear regression yields an $R^2$ value of 0.92, indicating that 92% of the variability in the dependent variable is explained by the independent variable. The equation Y=1.46x−15.40 (Fig 2.d) demonstrates a strong positive relationship between the variables. While this high $R^2$ value suggests a good fit, it is important to evaluate residual patterns and the statistical significance of the coefficients to ensure the model's robustness and avoid potential overfitting. Although this model is proposed, further validation will involve independent data that were not used during model development, followed by testing using log data to confirm its reliability and applicability.

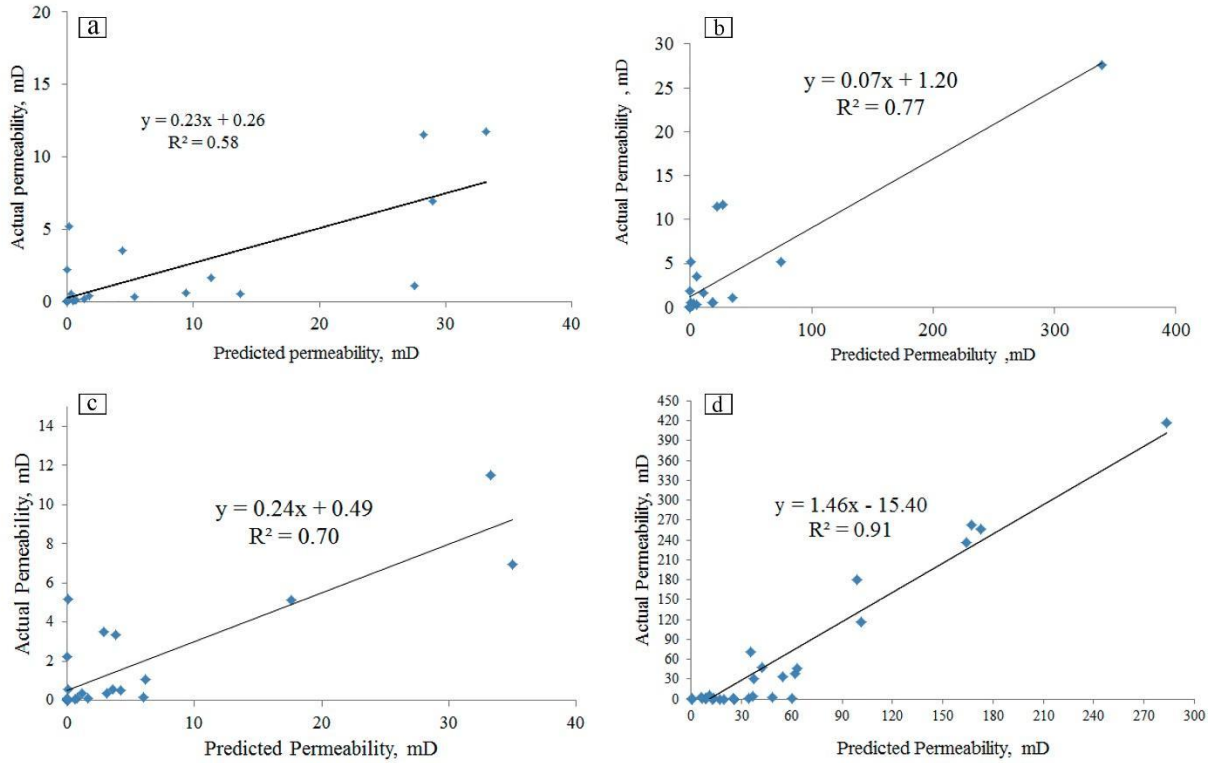

Fig. 2. Presentation of the measured permeabilities vs. their predicted values in Winland (a), Pitman (b), Swanson (c), and newly proposed model (d). The $R^2$ values and the slope of the lines and y-intercepts are also presented in each plot.

### 3.4 Verification of the Model by independent MICP data

MICP data from two additional wells were used to verify the new model. The samples for verification were from the same carbonate formations. Predicted permeability values were compared with the measured values, yielding satisfactory results. These results are presented in Fig. 3.

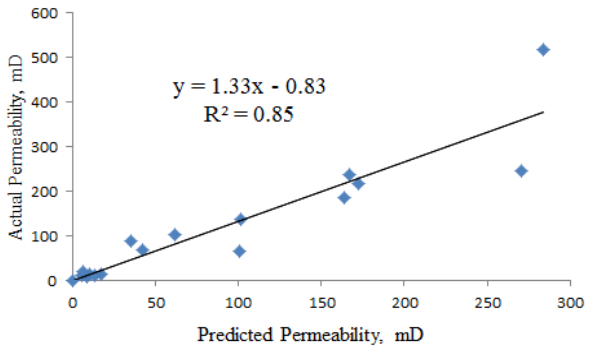


**Fig. 3**. Comparison of measured and predicted permeability values based on the new model.

### 3.5 Model verification using sonic log and Stoneley permeability

Permeabilities were also obtained using Stoneley waves, extracted from a sonic scanner in the reservoir. The permeability values derived from Stoneley waves showed a strong correlation with those obtained from modular formation dynamic tests (MDT). The results are presented in Fig.4.

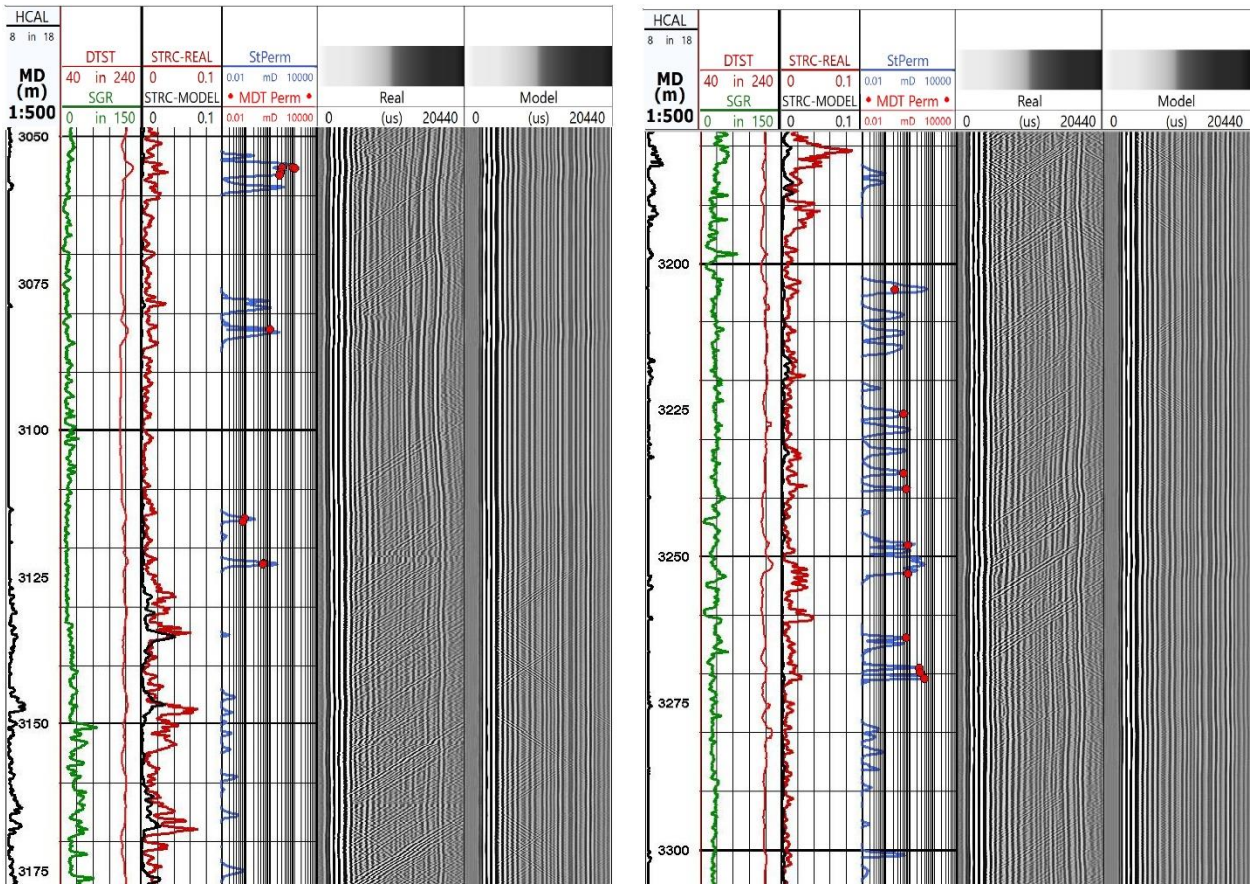

Fig. 4. Comparison of the generated permeability from Stoneley waves and MDT.

The next step involved comparing the permeability log, confirmed by MDT, with the predicted permeability from the new model. The result was satisfactory, with an $R^2$ value of 0.71, as shown in Fig. 5.

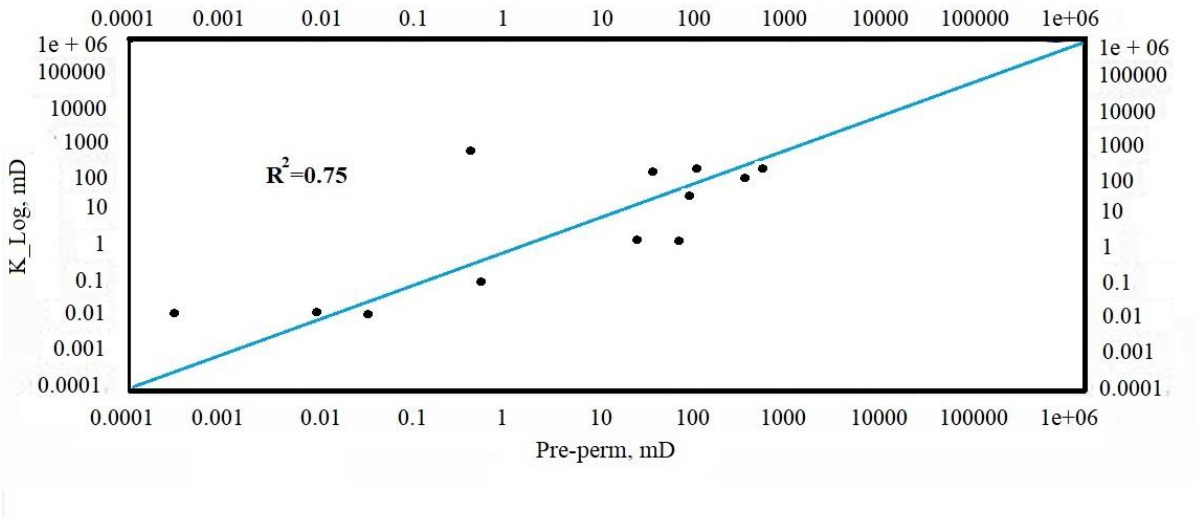


**Fig. 5**. Comparison of permeability derived from Stoneley waves and predicted permeability from the new model.

This study introduces a new empirical model for permeability prediction specifically tailored to carbonate rocks. By accounting for the heterogeneity inherent in various carbonate facies, the proposed model enhances the accuracy of permeability predictions. Existing experimental models, such as Winland's, often rely on core samples calibrated using both carbonate and clastic formations. However, due to significant differences in petrophysical properties between carbonate and clastic rocks, permeability predictions from these models may lack precision. These disparities, which can influence calcite solubility and subsequently permeability, add complexity to reservoir characterization. For instance, Winland's model averages petrophysical features across both rock types, potentially introducing inaccuracies, as reflected in the $R^2$ values shown in Fig. 2. Similarly, the Pitman and Swanson models, calibrated using clastic rocks, exhibit reduced reliability when applied to carbonate reservoirs.

In contrast, the proposed model accounts for the distinct characteristics of carbonate formations, considering the different facies and sedimentary environments that influence permeability. This

approach is particularly important for carbonate reservoirs, where geological features can vary significantly.

Different facies exhibit varying petrophysical characteristics, which influence permeability prediction. However, the proposed model incorporates samples from a range of facies with diverse petrophysical properties. Previous research (e.g., Nooruddin et al., 2014; Rashid and Glover, 2016) has demonstrated that earlier models sometimes yield significant errors. In the current model, the linear regression equation between predicted and measured permeability is characterized by a slope and an $R^2$ value. A slope and $R^2$ value of 1 indicate a close match between actual and predicted permeability. In the proposed model, the slope and $R^2$ values are 1.4 and 0.91, respectively. The new model incorporates more effective parameters, reducing the impact of errors in varying conditions. Key factors such as R35, porosity, and $Sb/Pc_{max}$ were specifically considered and adjusted for carbonate rocks. Other models were developed based on different formations, lithologies, and sedimentary environments. The permeability predictions from the proposed model, compared with actual permeability measurements, were reliable. Although the predictions were satisfactory, the model was further verified using data from different wells. The verification results showed a slope of 1.3 and an $R^2$ value of 0.85, indicating high accuracy in predicting permeability in these carbonate formations.

The model also demonstrated good agreement with modular formation dynamic tests (MDT), which reflect dynamic permeability under natural reservoir conditions. The comparison between the predicted permeability from the new model and the permeability log derived from Stoneley waves showed a strong correlation. These results indicate that accurate permeability data can be obtained under natural reservoir conditions.

## 4 Conclusions

This study presents a new empirical correlation for estimating permeability in carbonate reservoirs. The proposed model, developed using data from various carbonate formations, incorporates more effective parameters, resulting in improved permeability prediction. Future studies could explore the applicability of this model to other formations or investigate the effects of different geological parameter.

**Competing Interests and Funding**

The authors declare that they have no known competing financial interests or personal relationships that could have appeared to influence the work reported in this paper.

Declaration of generative AI and AI-assisted technologies in the writing process.

## 5 References


Bernabé, Y., Maineult, A., 2015. Physics of porous media: fluid flow through porous media. Treatise on Geophysics 19–41. http://dx.doi.org/10.1016/B978-0-444-53802-4.00188-3

Brooks, R.H., Corey, A.T., 1966. Properties of porous media affecting fluid flow. J. Irrig. Drain. Div. Proc. Am. Soc. Civ. Eng. 92(02), 61–88. https://oceanrep.geomar.de/id/eprint/47504

Burdine, N., 1953. Relative permeability calculations from pore size distribution data. J. Pet. Technol. 5(03), 71–78. https://doi.org/10.2118/225-G

Chen, Y., 2014. Convolutional neural network for sentence classification. University of Waterloo. https://doi.org/10.48550/arXiv.1408.5882

Comisky, J.T., Newsham, K.E., Rushing, J.A., Blasingame, T.A., 2007. A comparative study of capillary-pressure-based empirical models for estimating absolute permeability in tight gas sands. The SPE Annual Technical Conference and Exhibition. http://dx.doi.org/10.2523/110050-MS

Corey, A.T., 1954. The interrelation between gas and oil relative permeabilities. Prod. Mon. 19(01), 38–41. https://doi.org/10.3720/japt.78.243.

Dastidar, R., Sondergeld, C.H., Rai, C.S., 2007. An improved empirical permeability estimator from mercury injection for tight clastic rocks. Petrophysics 48(3), 186–190. https://www.webofscience.com/wos/WOSCC/full-record/000247157900003

Dixit, A.B., McDougall, S.R., Sorbie, K.S., et al., 1998. Analysis of relative permeability hysteresis trends in mixed-wet porous media using network models. In: SPE/DOE Improved Oil Recovery Symposium, Tulsa, Oklahoma, SPE-39656-MS. https://doi.org/10.1016/j.petrol.2017.11.014

Feng, D., Bakhshian, S., Wu, K., Song, Z., Ren, B., Li, J., Hosseini, S.A., Li, X., 2021. Wettability effects on phase behavior and interfacial tension in shale nanopores. Fuel 15(290), 119983. https://ui.adsabs.harvard.edu/link_gateway/2021Fuel..29019983F/doi:10.1016/j.fuel.2020.119983

Feng, D., Li, X., Wang, X., et al., 2018. Capillary filling under nanoconfinement: the relationship between effective viscosity and water-wall interactions. Int. J. Heat Mass Transf. 118, 900–910. https://doi.org/10.1016/j.ijheatmasstransfer.2017.11.049.

Gao, Z., Hu, Q., 2013. Estimating permeability using median pore-throat radius obtained from mercury intrusion porosimetry. J. Geophys. Eng. 10(2), 025014. https://doi.org/10.1088/1742-2132/10/2/025014

Glover, P.W., Zadjali, I.I., Frew, K.A., 2006. Permeability prediction from MICP and NMR data using an electrokinetic approach. Geophysics 71(4), F49–F60. https://doi.org/10.1190/1.2216930

Guo, B., Ghalambor, A., Duan, S., 2004. Correlation between sandstone permeability and capillary pressure curves. J. Petrol. Sci. Eng. 43(3), 239–246. http://dx.doi.org/10.1016/j.petrol.2004.02.016

Helba, A.A., Sahimi, M., Scriven, L.E., et al., 1992. Percolation theory of two-phase relative permeability. In: 57th Annual Fall Technical Conference and Exhibition of SPE, New Orleans, SPE 11015-PA. https://doi.org/10.2118/11015-PA.

Huet, C., Rushing, J., Newsham, K.E., Blasingame, T.A., 2005. A modified Purcell model for estimating absolute permeability from mercury injection capillary pressure data. The 2005 International Technology Conference, Doha, Qatar. https://doi.org/10.2523/IPTC-10994-MS.

Kadet, V.V., Galechyan, A.M., 2014. Percolation modeling of relative permeability hysteresis. J. Pet. Sci. Eng. 119, 139–148. https://doi.org/10.1016/j.petrol.2014.05.001.

Kamath, J., 1992. Evaluation of accuracy of estimating air permeability from mercury-injection data. SPE Form. Eval. 7(04), 304–310. https://doi.org/10.2118/18181-PA

Katz, A.J., Thompson, A.H., 1986. Quantitative prediction of permeability in porous rock. Phys. Rev. B 34, 8179–8181. https://doi.org/10.1103/physrevb.34.8179

Kolodize, S., 1980. Analysis of pore throat size and use of the Waxman-Smits equation to determine OOIP in Spindle Field. 55th Society of Petroleum Engineering Annual Technical Conference and Exhibition, Colorado, USA, 9382–9386. https://doi.org/10.2118/9382-MS

Krevor, S.C.M., Pini, R., Zuo, L., et al., 2012. Relative permeability and trapping of CO2 and water in sandstone rocks at reservoir conditions. Water Resour. Res. 48(2), W02532. https://doi.org/10.1029/2011WR010859.

Lanetc, Z., Zhuravljov, A., Armstrong, R.T., et al., 2024. Estimation of relative permeability curves in fractured media by coupling pore network modeling and volume of fluid methods. Int. J. Multiph. Flow 171, 104668. http://dx.doi.org/10.1016/j.ijmultiphaseflow.2023.104668

Liu, J.Q., Zhang, C.M., Zhang, Z., 2016. Combine the capillary pressure curve data with the porosity to improve the prediction precision of permeability of sandstone reservoir. J. Petrol. Sci. Eng. 139, 43–48. http://dx.doi.org/10.1016/j.petrol.2015.12.018

Nooruddin, H.A., Hossain, M.E., Al-Yousef, H., Okasha, T., 2014. Comparison of permeability models using mercury injection capillary pressure data on carbonate rock samples. J. Petrol. Sci. Eng. 121, 9–22. http://dx.doi.org/10.1016/j.petrol.2014.06.032

Phirani, J., Pitchumani, R., Mohanty, K., 2009. Transport properties of hydrate-bearing formations from pore-scale modeling. In: SPE Annual Technical Conference and Exhibition, New Orleans, Louisiana, SPE-124882-MS. https://doi.org/10.2118/124882-MS.

Pittman, E.D., 1992. Relationship of porosity and permeability to various parameters derived from mercury injection-capillary pressure curves for sandstone. AAPG Bull. 76(2), 191–198. https://doi.org/10.1306/BDFF87A4-1718-11D7-8645000102C1865D.

Purcell, W.R., 1949. Capillary pressures - Their measurement using mercury and the calculation of permeability therefrom. J. Petrol. Technol. 1, 39–48. https://doi.org/10.2118/949039-G.

Rezaee, M.R., Jafari, A., Kazemzadeh, E., 2006. Relationships between permeability, porosity, and pore throat size in carbonate rocks using regression analysis and neural networks. J. Geophys. Eng. 3(4), 370–376. https://doi.org/10.1088/1742-2132/3/4/008

Rezaee, R., Saeedi, A., Clennell, B., 2012. Tight gas sands permeability estimation from mercury injection capillary pressure and nuclear magnetic resonance data. J. Petrol. Sci. Eng. 88, 92–99. https://doi.org/10.1016/j.petrol.2011.12.014

Rezaei, M., Tavakoli, V., Rahimpour-Bonab, H., 2020. Comparison of different permeability estimation models based on pore throats. *J. Pet. Sci. Res.* **9**, 68–77. https://doi.org/10.22078/pr.2020.4142.2879.

Salomao, M.C., 1997. Analysis of flow in spatially correlated systems by applying the percolation theory. In: 15th Latin American and Caribbean Petroleum Engineering Conference, Rio de Janeiro, Brazil, SPE-39039-MS. https://doi.org/10.2118/39039-MS.

Schwartz, L.M., Sen, P.N., Johnson, D.L., 1989. Influence of rough surfaces on electrolytic conduction in porous media. Phys. Rev. B Condens. Matter 40(4), 2450–2458. https://doi.org/10.1103/physrevb.40.2450

Swanson, B.F., 1981. A simple correlation between permeabilities and mercury capillary pressures. J. Petrol. Technol. 33(12), 2498–2504. https://doi.org/10.2118/8234-PA

Thomeer, J.H.M., 1960. Introduction of a pore geometrical factor defined by the capillary pressure curve. J. Petrol. Technol. 12(03), 73–77. https://doi.org/10.2118/1324-G

Thomeer, J.H.M., 1983. Air permeability as a function of three pore-network parameters. J. Petrol. Technol. 35(04), 809–814. https://doi.org/10.2118/10922-PA

Washburn, E.W., 1921. Note on a method of determining the distribution of pore sizes in a porous material. Proc. Natl. Acad. Sci. U.S.A. 7, 115–116. https://doi.org/10.1073/pnas.7.4.115.

Xiao, L., Liu, D., Wang, H., Li, J., Lu, J., Zou, C., 2017. The applicability analysis of models for permeability prediction using mercury injection capillary pressure (MICP) data. J. Petrol. Sci. Eng. 156, 589–593. http://dx.doi.org/10.46690/capi.2022.05.02

Zhang, C., Cheng, Y., Zhang, C., 2017. An improved method for predicting permeability by combining electrical measurements and mercury injection capillary pressure data. J. Geophys. Eng. 14(1), 132–142. https://doi.org/10.1088/1742-2140/14/1/132

Zhou, X.H., Wang, H., McClure, J., et al., 2023. Inference of relative permeability curves in reservoir rocks with ensemble Kalman method. Eur. Phys. J. E 46(6), 44. https://doi.org/10.48550/arXiv.2305.01029